https://doi.org/10.48048/tis.2023.6639

Degradation of Ciprofloxacin (CIP) Antibiotic Waste using The Advanced Oxidation Process (AOP) Method with Ferrate (VI) from Extreme Base Electrosynthesis

Gunawan Gunawan*, Nor Basid Adiwibawa Prasetya and Roni Adi Wijaya

Department of Chemistry, Diponegoro University, Semarang 50275, Indonesia

(*Corresponding author's e-mail: gunawan@live.undip.ac.id)

Received: 18 January 2023, Revised: 12 February 2023, Accepted: 3 March 2023, Published: 20 March 2023

Abstract

Ciprofloxacin (CIP) antibiotic liquid waste is the most common waste found in hospital discharge waters. The accumulation of CIP can increase mutation, microbial resistance, and toxicity in the environment due to its low biodegradability and longevity in waters. Thus, methods for eliminating CIP are important. The Advanced Oxidation Process (AOP) method with ferrate (VI) has good redox potential in water disinfection, and degradation of organic and inorganic pollutants. Therefore, this study aims to degrade CIP waste with ferrate (VI). The ferrate (VI) used was synthesized from the electrolysis of transformer scrap metal plates under extremely alkaline conditions. The success of the synthesis was proven by the presence of FeO(OH) groups characterized using FTIR, XRF, and XRD. Then, the effect of time, pH, and CIP degradation was studied. The results showed that the maximum performance was obtained at pH 7 and 120 min with the addition of 1.1 mg ferrate at initial CIP concentration of 30 mg/L. The concentration of CIP decreased with increasing treatment time which was confirmed by UV-Vis Spectrophotometer. This condition is able to degrade 86.7 % of CIP. In addition, the LC-MS results show that degradation occurs due to a reaction between $HFeO_4^-/H_2FeO_4$ and the active site of piperazine ring antibiotics. This shows that Ferrate has a promising potential to reduce ciprofloxacin antibiotic pollution from hospital wastewater for a better environment.

Keywords: Ciprofloxacin, Antibiotic waste, Ferrate, Electrosynthesis, Waste degradation

Introduction

Global antibiotic consumption rates are projected to increase from 42.3 billion definite daily doses (DDD) in 2015 to 128 billion DDD in 2030, which equates to an increase of 15.8 DDD per 1,000 population each day [1]. Meanwhile, more than 58 % of antibiotics are excreted through urine and feces into the sewer system and surface water as waste [2]

Ciprofloxacin (CIP) wastewater is an antibiotic waste that is most often found in sewers, water bodies, and even in the effluent wastewater treatment plant (WWTP) of hospitals [3]. CIP tends to accumulate in the environment because of its low biodegradability [4] and long lifetime in water. CIP can also spread into the food chain through trophy transfer [5-7] increasing microbial resistance and toxicity is harmful to humans, environmental and human health [8]. Therefore, an effective method for eliminating CIP is important.

The current wastewater treatment method at the Wastewater Treatment Plant (WWTP) uses conventional biological and adsorption methods. However, biological method is not efficient in removing fused aromatic ring antibiotics, such as CIP [9]. Meanwhile, the absorption method [10] is only to absorb and transfer pollution to other forms of pollution in absorbent solid waste. While, the application of Advanced Oxidation Processes (AOPs) with ozone microbubbles [11], UV light [12], or catalysts, has been reported as a promising method for the oxidative removal of various organic contaminants in polluted water [13].

The basic principle of AOPs is that they generate reactive oxygen species (ROS), including oxygen ($\bullet O_2^-$), hydroxyl ($\bullet OH$), and hydroperoxyl radicals ($\bullet HO_2$) [14]. Among AOP-based methods, dielectric barrier discharge plasma (DBDP) and ozone are efficient green technologies for antibiotic degradation [15], DBDP and ozone have high operating costs, plasma conditioning which is complicated and requires external energy so it is impractical [16]. While photocatalysts are limited to operations with UV light. On the other hand, the use of Fe(VI), has emerged as an effective green oxidant to treat various contaminants in waters [17-19] mainly involving the degradation of dyes [20-22], removal of metal ions [23], degradation

of natural organic matter or disinfection by-products [24,25] at room temperature and without external energy. Ferrate(VI) is a very strong oxidant with a high redox potential of 2.2V, which is compatible with ozone (2.0 V) [26] and environmentally friendly [27]. Ferrates can produce hydroxyl radical groups (•OH) in an aqueous environment which can attack the quinolone groups of some antibiotics [28], so they also have a good potential in degrading CIP antibiotics.

Several studies related to antibiotic degradation such as ofloxacin [28], sulfamethoxazole [29], levofloxacin [30] with Fe (VI) have been successfully carried out. Feng *et al.* [31] have degraded the antibiotics enrofloxacin, norfloxacin, ofloxacin, and marbofloxacin with Fe (VI) from $FeCl_3$ in NaOCl. While Wang *et al.* [32] studied the effect of pH on the oxidation of fluoroquinolone antibiotics with Fe (VI) of K_2FeO_4 in $Na_2B_4O_7{\cdot}Na_2HPO_4$ buffer solution. However, the ferrate application in ciprofloxacin antibiotic degradation has never been done. Therefore, this study aims to conduct a study of the degradation of artificial waste antibiotics ciprofloxacin using ferrate from electrosynthesis in extremely bases. The ferrate used is obtained from the electrosynthesis of transformer iron waste in NaOH electrolytes. The success of ferrate synthesis is confirmed by FTIR, XRD, and XRF. Then it was applied ~~to~~ for CIP degradation with the effect of pH variations and treatment time observed. In addition, the effectiveness of degradation is measured using the UV-Vis spectrophotometer and the degradation mechanism is predicted with LC/MS. This research is expected to be a solution to the existing antibiotic waste problems, as well as develop the potential of ferrate synthesis from less utilized waste.

Materials and methods

Materials and equipment

The materials used in this study included ciprofloxacin, an iron anode plates from used transformers, zinc cathode plates, sodium hydroxide (NaOH, Merck pa), sodium hypochlorite (NaOCl, Merck pa), glass wool, and hydrochloric acid (HCl, Merck pa). The equipment used in this study were erlenmeyer (Herma), dropper pipettes (Herma), volumetric flasks (Herma), beakers (Pyrex), vials (Herma), glass funnels (Herma), burettes (Herma), states and clamps, watch glass (Herma), oven (Kirin), chamber equipped with a stirrer, filter paper (Whatman no. 42), analytical balance (Kern), thermometer, Digital DC power supply (Aditeg APS 3005), power supply with the regulator. The instruments used were FTIR spectrophotometer (Shimadzu IRPRESTIGE 21), X-Ray Diffractometers (Shimadzu XRD-6100/7000), LC-30A liquid chromatography (Shimadzu Co., Japan) and QTOF5600 mass spectrometry (AB Com., USA) with electrospray ionization source (EIS), X-ray Fluorescence (PANalytical XRF), as well as UV-Vis spectrophotometer (Genesys 10 S UV-Vis).

Synthesis of ferrate by electrolysis with extreme bases

Ferrate (VI) was obtained by electrolysis of a zinc cathode plate and an iron anode from a used transformer with dimension of 1.5×5 cm^2 using DC current. The electrodes were immersed in a beaker containing 50 mL of 14 M NaOH electrolyte with a potential of 3 V and a current of 4.28 A for 60 min in an ice vessel. After the electrolysis was complete, then 10 mL of NaOCl was added, and allowed to stand for 3 h. The electrolysis solution was filtered using glass wool to separate impurities.

Characterization of ferrate

The electrolyzed sodium ferrate solution was frozen for characterization purposes. The solution was frozen at −70 °C in a freeze dryer for 12 h to give solid Na_2FeO_4. The ferrate solid samples were then characterized using FTIR (Shimadzu IRPRESTIGE 21) to determine the presence of functional groups and chemical bond structures. The crystalline phase of the sample was examined with an X-ray diffractometer (XRD) (Shimadzu XRD-6100/7000), with Cu Kα radiation (1.5406 A) at an angle of 20 - 60 ° and metal composition with XRF (PANalytical XRF).

CIP artificial waste preparation and calibration

The 100 mg/L ciprofloxacin mother liquor was obtained from 0.01 g of ciprofloxacin purity 98 % dissolved in 100 mL of distilled water. The solution was stirred with a magnetic stirrer at 400 rpm for 600 min. CIP's artificial waste was conditioned as in the WWTP effluent of hospital liquid waste, made from diluting the mother liquor into distilled water at a ratio of 1:99 so that the initial volume of ciprofloxacin liquid waste was 100 mL [33]. The stock solution of ciprofloxacin 100 mg/L was diluted into various concentrations of 10, 15, 20, 25, and 30 mg/L with distilled water for calibration purposes. Then the absorbance was observed using a UV-Vis spectrophotometer (Genesys 10 S UV-Vis) at 270 - 400 nm.

CIP degradation with ferrate with the variation of pH

CIP degradation was carried out by adding 1.1 mg ferrate to 30 mg/L ciprofloxacin solution at varying pH for 60 min. Variation conditioning was carried out by adding HCl to the sample resulting from electrolysis until a variation of pH 3, 7, and 10 were obtained. Then the absorbance was measured by using a UV-Vis spectrophotometer.

CIP degradation with ferrate treatment time variation

The effect of variations in treatment time on degradation was carried out by periodic observations at 10, 30, 60, and 120 min at pH 7. The results of each degradation time were observed by using a UV-Vis spectrophotometer.

Determination of the mechanism of the degradation reaction

The mechanism of CIP degradation was identified by LC-MS using an LC-30A liquid chromatography (Shimadzu Co., Japan) and QTOF5600 mass spectrometry (AB Com., USA) with an electrospray ionization source (EIS). The sample used was ciprofloxacin 30 mg/L with 1.1 mg ferrate at pH 7 with a treatment time of 120 min. Sample pretreatment was performed with a vortex mixer (Thermo Fisher Scientific, Waltham, MA, USA) and a high-speed cooled centrifuge (Tomy MX-200, Thermo Fisher Scientific). While data processing was done by MassHunter B.07.00 workstation.

Results and discussion

Synthesis of ferrate

The synthesis of ferrate by electrolysis at extreme bases was carried out using a used transformer iron plate electrode as the anode, zinc as the cathode, and 14 M NaOH solution as the electrolyte. Next, electrolysis was carried out with a constant voltage of 4 V and a current reading of 4.28 A. This electrolysis method is the easiest way to obtain sodium ferrate in a solution without impurities [34]. The resulting Na_2FeO_4 solution was filtered using glass wool to remove the precipitate in the solution. The oxidation-reduction reaction of the electrolysis of the iron plate that occurs is expressed in reaction (1) as follows:

$$\begin{aligned} &\text{Anode} && : Fe + 8\ OH^- \leftrightarrow FeO_4^{2-} + 4\ H_2O + 6\ e^- \\ &\underline{\text{Katode}} && \underline{: 6\ H_2O + 6\ e^- \leftrightarrow 3\ H_2 + 6\ OH^-} \\ &\text{Result} && : Fe + 2\ OH^- + 2\ H_2O \rightarrow FeO_4^{2-} + 3\ H_2 \end{aligned} \quad (1)$$

Ferrate (VI) is unstable in ionic form, and stable in salt form under alkaline conditions [21]. So that in the reaction there is an interaction with the NaOH electrolyte to form Na_2FeO_4 as in reaction 2. This result was also confirmed by the results of crystal characterization on XRD, FTIR and XRF.

$$FeO_4^{2-} + 3H_2 + 2NaOH \rightarrow Na_2FeO_4 + 3H_2 + 2OH^- \quad (2)$$

Characterization of Ferrate

The characterization of ferrate powder with FTIR confirmed the success of electrolysis in the presence of a functional group of Fe(VI) compounds as shown in the spectra of **Figure 1**. At the peaks of 1640, 2886 and 3573 cm^{-1} appeared as OH vibrational strains from water [35-37]. This is because ferrate powder is hygroscopic. The absorption at 1434 cm^{-1} is characteristic of the stretching vibration of the C-O bond, which is the peak of CO_2 in the air. While the sharp peak in the fingerprint region shows the stretching vibration of the Fe-O bond at around 624, 779, and 879 cm^{-1} [21,38,39].

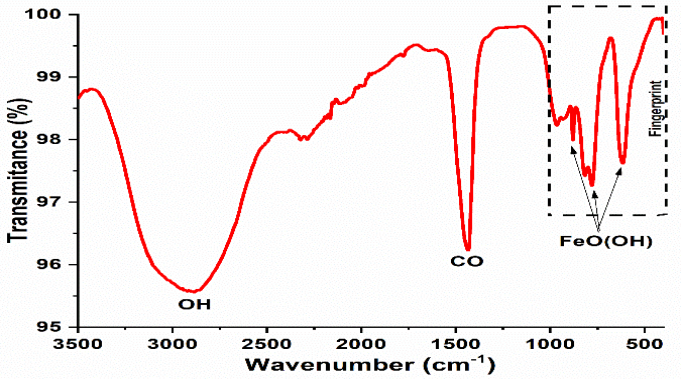

Figure 1 IR spectra of electrolyzed ferrate.

The ferrate powder was analyzed by XRD at 2-theta (2θ) between 20.00 - 60.00 ° with a CuK radiation diffractometer. The results in **Figure 2** show the presence of an isomorphic ferrate crystal structure as confirmed by the literature of Gunawan *et al.* [20] and Munyengabe *et al.* [40]. Sharp peaks of Na_2FeO_4 salt crystals were observed to appear at 27.27, 30.05, 35.14, 39.36, 40.51, 45.35 and 54.30 °. These results indicate that the crystal structure pattern of ferrate has orthorhombic properties and shows isomorphism with Na_2FeO_4 as found by Maghraoui *et al.* [41]. In addition, it is also found in the FeO(OH) phase at 25.53, 36.87, 47.13 and 48.80 ° according to (JCPDS no 34-1266) [21].

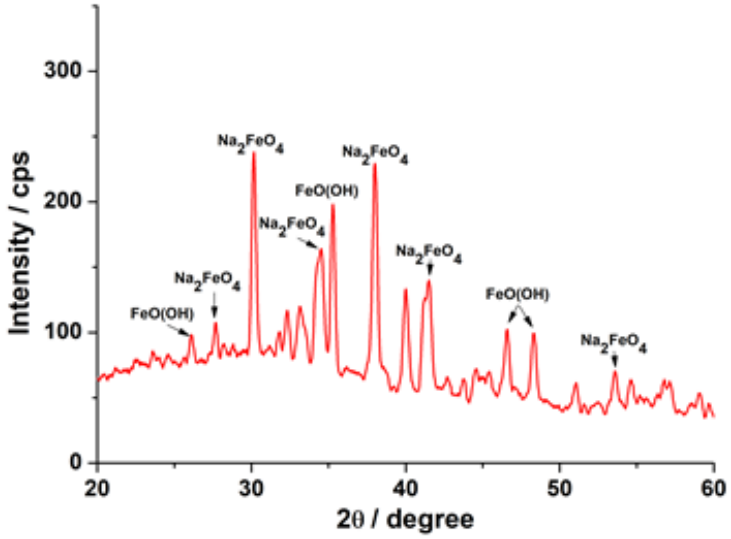

Figure 2 XRD Diffractogram of electrolyzed ferrate.

The test results for electrolyzed ferrate powder composition are shown in **Figure 3**. Most of the element iron (Fe) was found in its oxide form (Na_2FeO_4) as some of the previous studies [19-21]. Other compositions such as Sodium (Na) were also found in the remaining NaOH electrolyte ions used. Si, Ca, Ag, and K elements come from the preparation of analytical instruments. While Cl comes from the remaining addition of hypochlorite and zinc (Zn) comes from the cathode plate used during electrolysis.

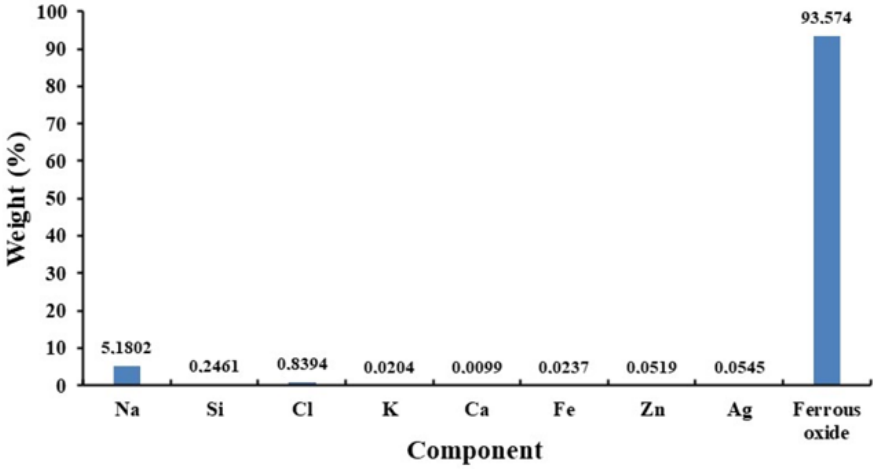

Figure 3 Components of ferrate powder elements resulting from electrolysis

CIP preparation and calibration

Two absorbance peaks of ciprofloxacin are obtained at a wavelength of 323 nm; and 334 nm in **Figure 4**. These results are in agreement with the literature of Kowalczuk *et al.* [42] and Woziwodzka *et al.* [43]. In this method, a series of ciprofloxacin concentrations are measured using the UV-Visible spectrophotometer to create a calibration curve. The absorbance absorption curve shows linear compatibility with the increase in CIP concentration.

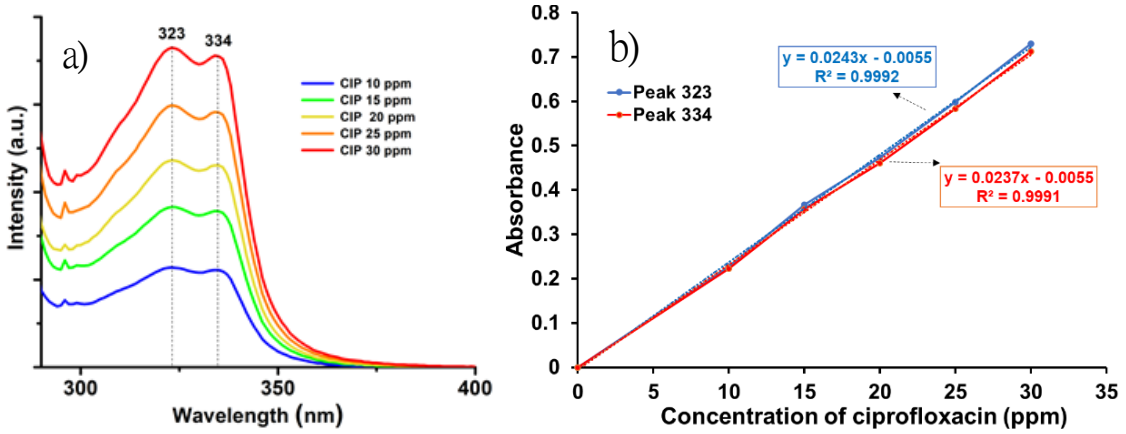

Figure 4 CIP absorbance of concentration variation (a) and calibration curve (b).

The best linearity test between absorbance vs ciprofloxacin concentration at a wavelength of 323 nm gave the determinant value of linearity $R^2 = 0.9992$ and the average molar extension value (ε) was 8.82×10^4 L mol^{-1} cm^{-1} which was interpreted through the gradient value or line slope, which was 0.0243 (±0.0055) compared to 334 nm which has $R^2 = 0.9991$ and a line slope of 0.0237 (±0.0055) with an average molar extension value (ε) of 8.59×10^4 L mol^{-1} cm^{-1}. Therefore, the wavelength of 323 nm was chosen as a reference in quantifying ciprofloxacin in the study sample. In addition, this value was also compared with other literature spectrophotometric methods which are listed in **Table 1** for determination of ciprofloxacin. As can be seen, the results of this study show that in terms of molar absorptivity (ε) it is in the same range as previous studies and even tends to be larger in several studies [44-46] and is close to the largest result [47], making it possible to perform analysis accurately at low concentrations of ciprofloxacin.

Table 1 Comparison molar extension value (ε) for the determination of ciprofloxacin.

λ max (nm)	ε (L mol^{-1} cm^{-1})	Reference
376	1.27×10^4	[44]
477	2.66×10^4	[45]
517	2.83×10^4	[46]
335	2.9×10^5	[47]
334	8.59×10^4	This work
323	8.82×10^4	This work

The prepared CIP artificial waste has an absorption area in the ultraviolet (UV) region. The UV-Vis spectrum of CIP as shown in Figure 5 shows 2 distinct peaks at 323 and 334 nm, which arise due to $\pi \rightarrow \pi*$ transitions of the fluorobenzene moieties (a) and quinolone ring (b), respectively [48]. The addition of ferrate (VI) seemed to change the absorption peak to one. This phenomenon is in line with several previous studies of CIP degradation by various media such as by Thakur *et al.* [48] which showed a decreased peak, especially at the peak of the quinolone ring associated with the piperazinyl group in the red circle in Figure 5. So the curve changes after the addition of ferrate due to changes in the existing CIP structure, wherein the initial mechanism there is an attack on the active side of piperazinyl which causes the absorption of the quinolone ring group (b) to become sloping and disappear.

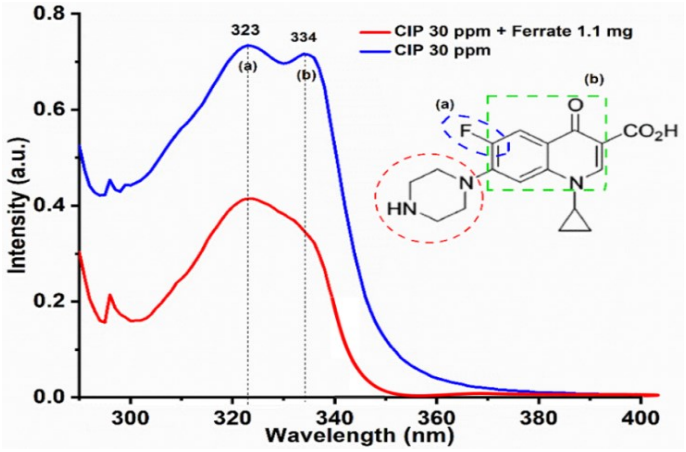

Figure 5 CIP absorbance curve.

Further analysis can be estimated by modeling as done by Serna-Garvis *et al.* [49] that modeled the 3D structure of ciprofloxacin reactive points through topological analysis with the Fukui Function as shown in **Figure 6**. Based on these simulations it is known that the piperazinyl region has a large electron density making it susceptible to attack by free radicals such as •OH and ozone (O_3) [49,50]. The reaction of breaking the C-F atomic bond in the fluorine group requires greater energy than the energy needed to break the C-H or C-N bonds [51].

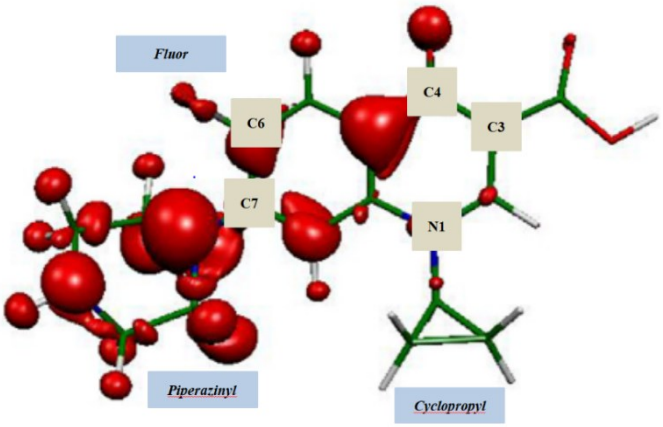

Figure 6 Theoretical study of the ciprofloxacin reactive area (red color) by topological analysis.

CIP degradation with ferrate pH variation

In this research, the effect of pH on the degradation of CIP with ferrate was studied as shown in Figure 7. The optimum results were obtained at pH 7 or nearly neutral. In this study, ferrates could degrade CIP as much as 26.23 mg/L with degradation effectiveness of 78.2 %. The rate of degradation increased to a peak at pH 7.0 and then decreased [39]. In addition, HO• can be an active species during Fe(VI) self-decay at pH 7.0 [32]. Meanwhile, HO• is rarely produced by self-decaying Fe(VI) under acidic and basic conditions. Schematically the reaction of the oxygen atom can lead to the production of a series of free radicals (Equations (3) and (4)) during the oxidation of Fe(VI) [52].

$$2\ FeO_4^{2-} + 4H_2O \longrightarrow 2\ Fe(OH)_3 + 4\ [O] + 2\ OH^- \quad (3)$$

$$[O] + H_2O \longrightarrow 2\ HO\bullet \quad (4)$$

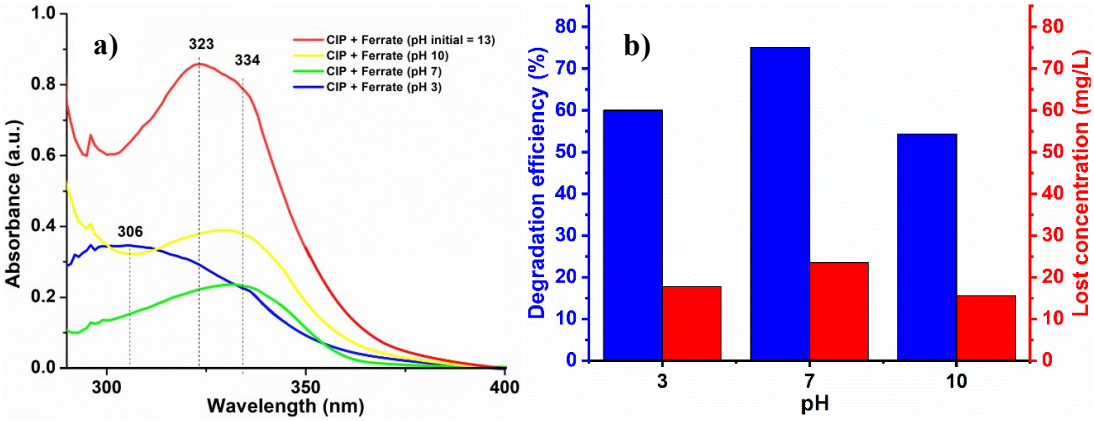

Figure 7 a) CIP absorbance reduction curve, and b) degradation effectiveness at various pH.

Besides affecting the results of degradation, pH also affects the absorption spectra of Ciprofloxacin. The maximum absorbance peak shifted to 306 nm at pH 3. The observable hypsochromic shift for ciprofloxacin at this change in pH was due to the deprotonation of the carboxylic and piperazine groups [53,54]. As an amphoteric fluoroquinolone antibacterial agent, CIP has a zwitterionic functional group, namely a positively charged piperazine group and a negatively charged carboxyl group as shown in Figure 9, which can affect its physical and chemical properties. In acidic (pH < pKa = 5.9) or basic (pH > pKa = 8.86) solutions, CIP is protonated or deprotonated. On the other hand, at neutral pH, CIP can reach equipotential points [55], so it can experience rapid degradation. HO• plays a role in the attack on the piperazine ring in CIP. So, in neutral pH conditions, more oxygen is produced and produces H_2O and the more active sites of CIP are degraded.

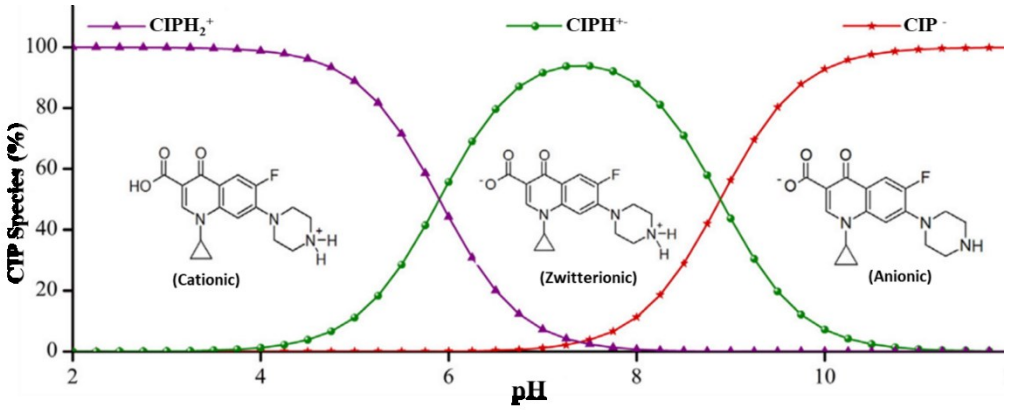

Figure 8 Distribution of CIP species as a function of pH.

CIP degradation with ferrate treatment time variation

Figure 9 presents the degradation curve of ciprofloxacin by ferrate. The degradation of ciprofloxacin depends on the duration of treatment (time-dependent), which shows that the duration of treatment is inversely proportional to the concentration of ciprofloxacin at a certain time. This is because the longer the reaction time, the more contact occurs between the ferrate and the active group of piperazine in ciprofloxacin. In this study, it was found that ferrate within 120 min could degrade CIP by 30 mg/L with 86.7 % effectiveness.

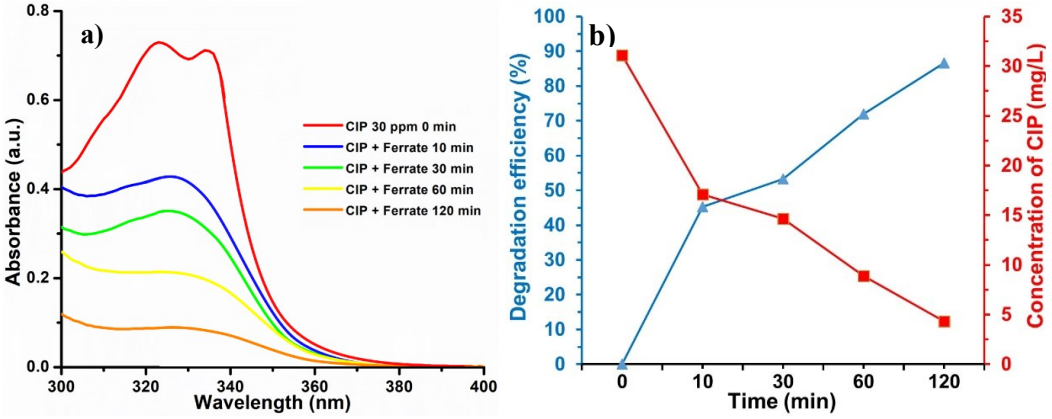

Figure 9 a) CIP absorbance reduction curve, and b) degradation effectiveness at various times.

A comparison of this study with several ciprofloxacin degradation methods is shown in **Table 2**. It can be seen that the effect of this method tends to have a better degradation efficiency than photocatalytic [12,56] and Fenton oxidation [57], ozonation microbubble [11] and lower than the ozonation system [58]. However, if we look in more detail at ozonation by Wajahat *et al.* [58], the initial concentration is too small, namely, 7.9 mg/L, while in this study it was able to effectively achieve ciprofloxacin degradation at high ciprofloxacin concentrations, namely 30 mg/L. In addition, degradation with ferrates can be carried out at room temperature, making it easier to observe.

Table 2 Comparison degradation efficiency by different methods.

Methods	Material	Degradation conditions	Degradation efficiency (%)	Reference
Advanced Oxidation Process (AOP)	Fe (VI)	pH = 7, initial concentration = 30 mg/L	86.7	This work
Photocatalytic	3D γ-Fe_2O_3@ZnO	pH = 3.5, initial concentration = 15 mg/L	18.30	[12]
Photocatalytic	Bi_2WO_6/Ag/AgBr	pH = 7, initial concentration = 50 µg/L	57%	[56]
Fenton oxidation	Fe^{2+}/H_2O_2	pH = 3.5, initial concentration = 15 mg/L	74.40	[57]
Ozonation	Ozone	pH = 9, initial concentration = 7.91 mg/L	98.7	[58]
Ozonation microbubbles	Ozone	pH = 7, concentration = 10.94 mg/L	83.5	[11]

Determination of the mechanism of the degradation reaction

Chromatogram results from LC-MS analysis of ciprofloxacin degradation products with ferrate (VI) have several peaks with different retention times as shown in **Figure 10** and **Table 3**. N and O atoms in ciprofloxacin are able to donate their lone pair to Fe (VI) to form complex compounds. In general, ciprofloxacin complexes with metals are formed in the carbonyl group on the piperazine ring [59].

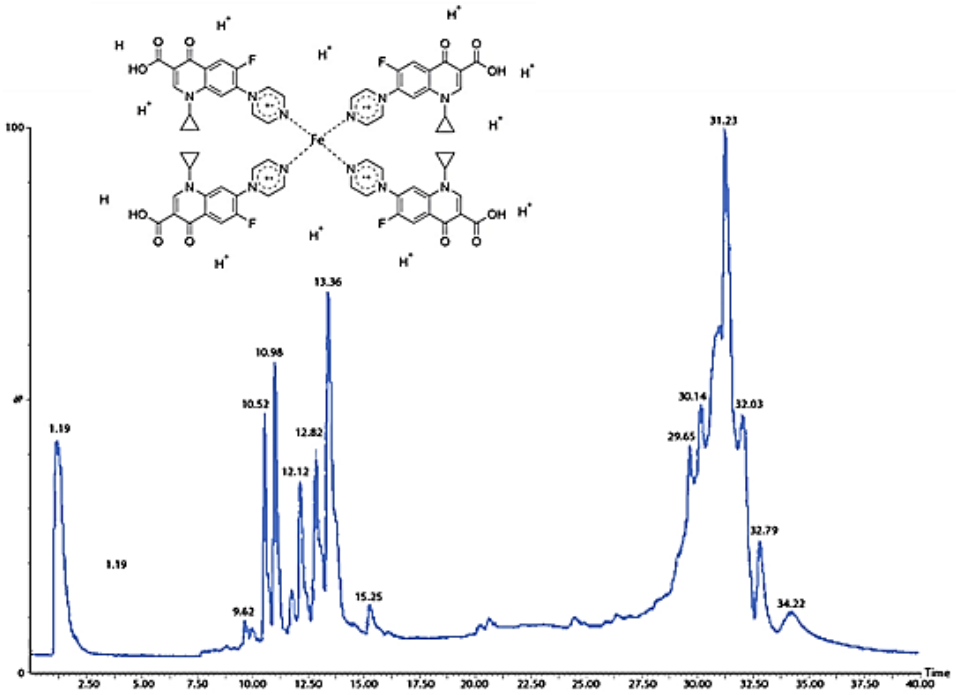

Figure 10 Chromatogram of degradation ciprofloxacin product by Ferrate

Table 3 CIP degradation product molecules with Fe(VI).

Retention time	Structure	Formula	Reference
1.19	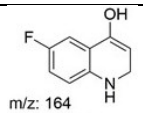 m/z: 164	C_9H_8FNO	[60]
9.62	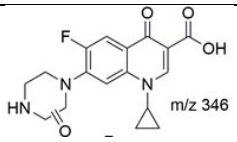 m/z 346	$C_{17}H_{18}FN_3O_4$	[61]
10.52	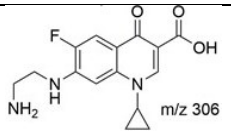 m/z 306	$C_{15}H_{16}FN_3O_3$	[61]
10.98	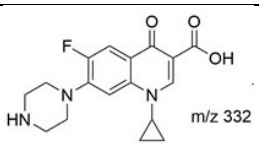 m/z 332	$C_{17}H_{18}FN_3O_3$	[61]
12.12	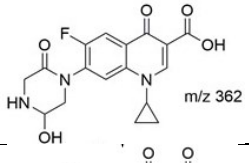 m/z 362	$C_{17}H_{16}FN_3O_3$	[61]
12.82	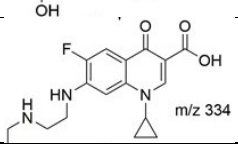 m/z 334	$C_{17}H_{20}FN_3O_3$	[62]

Retention time	Structure	Formula	Reference
13.36	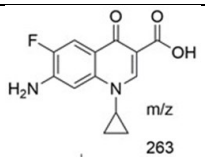	$C1_3H_{11}FN_2O_3$	[61]
15.25	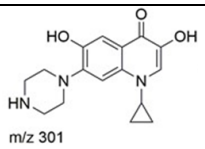	$C_{16}H_{19}N_3O_3$	[63]
31.23	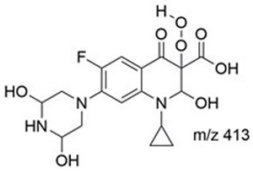	$C_{17}H_{20}FN_3O_8$	[60]
32.79	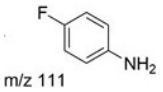	C_6H_6FN	[64]
34.22	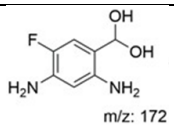	$C_7H_9FN_2O_2$	[65]

Based on the LC-MS chromatogram in **Figure 10**, it can be interpreted that the mechanism of CIP degradation by Fe(VI) is through the degradation pathway as shown in **Figure 11** by producing several products. The degradation was initiated by the attack on the unstable piperazine ring by •OH resulting from the ferrate reaction to form compound A with m/z 413 at retention times of 31.2 and 32.03 [60]. The increasing number of electrons in the piperazine ring causes the OH group to be oxidized to produce compound B with m/z 346 [61]. Meanwhile, if the reaction is further along with the increasing number of •OH which is produced by ferrate, it will cause fluorine substitution by the OH group and produce compound C with m/z 301 [63].

The resulting compound B is degraded in 2 possible ways. The first way is that compound B is reoxidized to compound D which has m/z 362 then undergoes reduction and rapid deformation of repeated actions to produce compound F with a value of m/z 306 [61]. In contrast to the second pathway, the piperazine ring of compound B undergoes a deformation reaction which is then followed by a hydrogenation reaction. This reaction causes the breaking of the amine bond (C−N) in the piperazine ring to produce compound E (m/z 334) [62]. The carbon chain in compound E undergoes a dissolution reaction of the 2 amine atoms (C−N) to produce compound F. Both processes of splitting the piperazine ring can break the amine bond (C-N) to produce compound G with m/z 263 [61].

Based on the existing product, compound G can then be degraded in 2 possible ways. The first pathway, through deamination reactions, decyclopropylization [66], and reduction or decarboxylation reactions produces compound H with m/z 164 [60]. Whereas in lane 2, degradation occurs through the loss of lateral groups in compound G resulting in compound I with m/z 172 [65]. The resulting compound I then undergoes deamination and decarboxylation reactions to produce compound J with m/z 111 [64]. Finally, from the mechanism that has been described, the prediction of the mechanism of the CIP degradation pathway by ferrate via pathway 2 that is more dominant or more recommended, this is based on the percent chromatogram product which dominates and the yield of simpler molecular products.

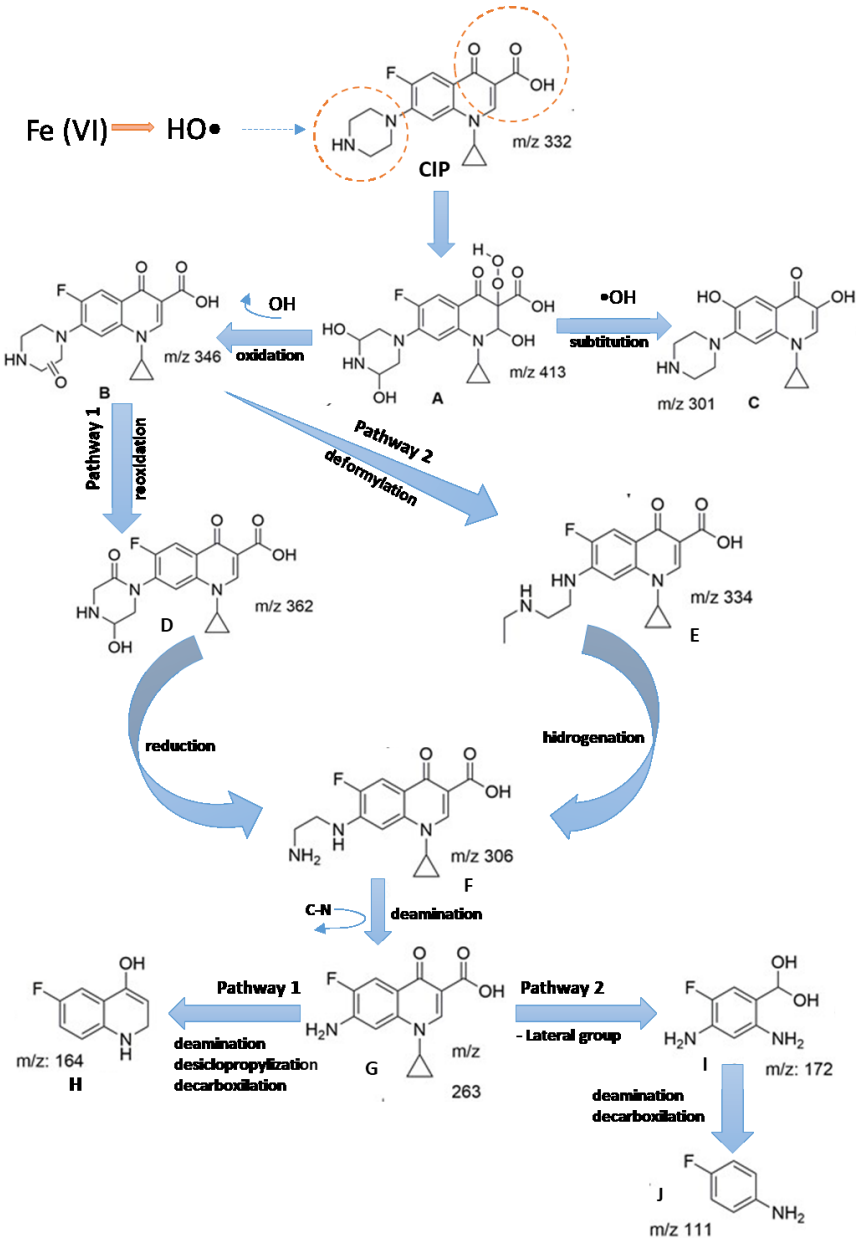

Figure 11 CIP degradation pathway by ferrate.

Conclusions

Artificial ciprofloxacin waste has been successfully degraded with ferrate produced from electrolysis in extreme bases. The ferrate used is synthesized from the electrolysis of transformer iron waste in NaOH solution. The success of synthesis is evidenced by the presence of FeO(OH) groups on FTIR, XRF, and XRD. The performance of ferrate for CIP degradation is influenced by pH and treatment time. The results showed that the maximum performance was obtained at pH 7 and 120 min with an additional dose of 1.1 mg of ferrate at the initial CIP concentration of 30 ppm. CIP concentration decreases over time the treatment confirmed by the UV-Vis spectrophotometer. This condition can reduce 86.2 % CIP. In addition, the LC-MS results show that degradation occurs due to a reaction between $HFeO_4^-/H_2FeO_4$ and the active site of piperazine ring antibiotics. This shows that ferrate has a promising potential to reduce ciprofloxacin antibiotic pollution from hospital wastewater for a better environment.

Acknowledgements

The authors are thankful to the RPP-Universitas Diponegoro, Indonesia 2022 for funding this work.

References

[1] EY Klein, TPV Boeckel, EM Martinez, S Pant, S Gandra, SA Levin, H Goosens and R Laxminarayan. Global increase and geographic convergence in antibiotic consumption between 2000 and 2015. *Proc. Natl. Acad. Sci.* 2018; **15**, 3463-70.

[2] SI Polianciuc, AE Gurzău, B Kiss, MG Ștefan and F Loghin. Antibiotics in the environment: Causes and consequences. *Med. Pharm. Rep*. 2020; **3**, 231.

[3] P Guerra, M Kim, A Shah, M Alaee and SA Smyt. Occurrence and fate of antibiotic, analgesic/antiinflammatory, and antifungal compounds in five wastewater treatment processes. *Sci. Total Environ.* 2014; **1**, 235-43.

[4] B Nas, T Dolu and S Koyuncu. Behavior and removal of ciprofloxacin and sulfamethoxazole antibiotics in three different types of full-scale wastewater treatment plants: A comparative study. *Water Air Soil Pollut*. 2021; **4**, 1-15.

[5] L Huang, Y Mo, Z Wu, S Rad, X Song, H Zeng, S Bashir, B Kang and Z Chen. Occurrence, distribution, and health risk assessment of quinolone antibiotics in water, sediment, and fish species of Qingshitan reservoir, South China. *Sci. Rep.* 2020; **1**, 1-18.

[6] SW Hyung, J Lee, SY Baek, S Lee, J Han, B Kim, K Choi, S Ahn, DK Lim and H Lee. Method improvement for analysis of enrofloxacin and ciprofloxacin in chicken meat: Application of in-sample addition of trace ethylenediaminetetraacetic acid to isotope dilution ultra-performance liquid chromatography-mass spectrometry. *Chromatographia* 2022; **1**, 35-45.

[7] S Keerthanan, C Jayasinghe, JK Biswas and M Vithanage. Pharmaceutical and personal care products (PPCPs) in the environment: Plant uptake, translocation, bioaccumulation, and human health risks. *Crit. Rev. Environ. Sci. Tech*. 2021; **12**, 1221-58.

[8] IC Stanton, AK Murray, L Zhang, J Snape and WH Gaze. Evolution of antibiotic resistance at low antibiotic concentrations including selection below the minimal selective concentration. *Commun. Biol.* 2020; **1**, 1-11.

[9] LF Zhai, HY Guo, YY Chen, M Sun and S Wang. Structure-dependent degradation of pharmaceuticals and personal care products by electrocatalytic wet air oxidation: A study by computational and experimental approaches. *Chem. Eng. J.* 2021; **423**, 130167.

[10] EWES Shahrin, NAH Narudin, NNM Shahri, M Nur, JW Lim, MR Bilad, AH Mahadi, J Hobley and A Usman. A comparative study of adsorption behavior of rifampicin, streptomycin, and ibuprofen contaminants from aqueous solutions onto chitosan: Dynamic interactions, kinetics, diffusions, and mechanisms. *Emerg. Contam*. 2023; **9**, 100199.

[11] SB Verinda, M Muniroh, E Yulianto, N Maharani, G Gunawan, NF Amalia, J Hobley, A Usman and M Nur. Degradation of ciprofloxacin in aqueous solution using ozone microbubbles: Spectroscopic, kinetics, and antibacterial analysis. *Heliyon* 2022; **8**, e10137.

[12] N Li, J Zhang, Y Tian, J Zhao, J Zhang and W Zuo. Precisely controlled fabrication of magnetic 3D γFe2O3@ZnO core-shell photocatalyst with enhanced activity: Ciprofloxacin degradation and mechanism insight. *Chem. Eng. J.* 2017, **308**, 377-85.

[13] DB Miklos, C Remy, M Jekel, KG Linden, JE Drewes and U Hübner. Evaluation of advanced oxidation processes for water and wastewater treatment - A critical review. *Water Res*. 2018; **139**, 118-31.

[14] K Shang, R Morent, N Wang, Y Wang, B Peng, N Jiang, N Lu and J Li. Degradation of sulfamethoxazole (SMX) by water falling film DBD Plasma/Persulfate: Reactive species identification and their role in SMX degradation. *Chem. Eng. J.* 2022; **431**, 133916.

[15] RC Sanito, SJ You and YF Wang. Degradation of contaminants in plasma technology: An overview. *J. Hazard. Mater*. 2022; **424**, 127390.

[16] EM Cuerda-Correa, MF Alexandre-Franco and C Fernández-González. Advanced oxidation processes for the removal of antibiotics from water: An overview. *Water* 2019; **1**, 102.

[17] B Yang, GG Ying, JL Zhao, S Liu, LJ Zhou and F Chen. Removal of selected endocrine disrupting chemicals (EDCs) and pharmaceuticals and personal care products (PPCPs) during ferrate(VI) treatment of secondary wastewater effluents. *Water Res*. 2012; **7**, 2194-204.

[18] JQ Jiang. Advances in the development and application of ferrate(VI) for water and wastewater treatment. *J. Chem. Tech. Biotechnol.* 2014; **2**, 165-77.

[19] VK Sharma, R Zboril and RS Varma. Ferrates: Greener oxidants with multimodal action in water treatment technologies. *Acc. Chem. Res*. 2015; **2**, 182-91.

[20] Gunawan, NBA Prasetya, A Haris and F Febriliani. Synthesis of ferrate using NaOCl and $Fe(OH)_3$ from electrolysis of used iron, and its application for metanil yellow degradation. *J. Phys. Conf. Ser.* 2021; **1943**, 012181.
[21] Gunawan, NBA Prasetya and RA Wijaya. Electrochemical synthesis of ferrate (FeO_4^{2-}) in extreme alkaline medium and its application in dye degradation. *Asian J. Chem.* 2022; **34**, 3361-68
[22] G Gunawan, NBA Prasetya, A Haris and E Pratista. Ferrate synthesis using NaOCl and its application for dye removal. *Open Chem*. 2022; **20**, 1142-54.
[23] G Gunawan, A Haris, NBA Prasetya, E Pratista and A Amrullah. Ferrate(VI) synthesis using $Fe(OH)_3$ from waste iron electrolysis and its application for the removal of metal ions and anions in water. *Indones. J. Chem.* 2021; **34**, 3361-8.
[24] W Gan, VK Sharma, X Zhang, L Yang and X Yang. Investigation of disinfection byproducts formation in ferrate(VI) pre-oxidation of NOM and its model compounds followed by chlorination. *J. Hazard. Mater.* 2015; **292**, 197-204.
[25] Y Jiang, JE Goodwill, JE Tobiason and DA Reckhow. Impacts of ferrate oxidation on natural organic matter and disinfection by product precursors. *Water Res*. 2016; **96**, 114-25.
[26] JQ Jiang, and B Lloyd. Progress in the development and use of ferrate (VI) salt as an oxidant and coagulant for water and wastewater treatment. *Water Res.* 2002; **6**, 1397-408.
[27] ZY Zhang, D Ji, W Mao, Y Cui, Q Wang, L Han and T Li. Dry chemistry of ferrate (VI): A solvent-free mechanochemical way for versatile green oxidation. *Angew. Chem. Int. Ed.* 2018; **34**, 10949-53.
[28] Y Chen, Q Jin and Z Tang. Degradation of ofloxacin by potassium ferrate: Kinetics and degradation pathways. *Environ. Sci. Pollut. Res.* 2022; **29**, 44504-12.
[29] B Jebalbarezi, R Dehghanzadeh, S Sheikhi, N Shahmahdi, H Aslani and A Maryamabadi. Oxidative degradation of sulfamethoxazole from secondary treated effluent by ferrate (VI): Kinetics, by-products, degradation pathway and toxicity assessment. *J. Environ. Health Sci. Eng.* 2022; **1**, 205-18.
[30] Q Jin, D Ji, Y Chen, Z Tang and Y Fu. Kinetics and pathway of levofloxacin degradation by ferrate (VI) and reaction mechanism of catalytic degradation by copper sulfide. *Sep. Purif. Tech.* 2022; **282**, 120104.
[31] M Feng, X Wang, J Chen, R Qu, Y Sui, L Cizmas, Z Wang and VK Sharma. Degradation of fluoroquinolone antibiotics by ferrate(VI): Effects of water constituents and oxidized products. *Water Res*. 2016; **103**, 48-57.
[32] D Wang, Z Zeng, H Zhang, J Zhang and R Bai. How does pH influence ferrate(VI) oxidation of fluoroquinolone antibiotics? *Chem. Eng. J.* 2022; **431**, 133381.
[33] C Sarangapani, Y Dixit, V Milosavljevic, C Sullivan, P Bourke and P Cullen. Optimization of Atmospheric air plasma for degradation of organic dyes in wastewater. *Water Sci. Tech.* 2017; **75**, 207-19.
[34] A El Maghraoui, A Zerouale, M Ijjaali, M Sajieddine, M ben Abdellah and M Fes. Synthesis and characterization of Ferrate(VI) alkali metal by electrochemical method. *Adv. Mater. Phys. Chem.* 2013; **1**, 83-7.
[35] L Macera, G Taglieri, V Daniele, M Passacantando and F D'orazio. Nano-Sized Fe(III) Oxide Particles Starting from an Innovative and Eco-Friendly Synthesis Method. *Nanomaterials* 2020; **2**, 323.
[36] BS Zhu, Y Jia, Z Jin, B Sun, T Luo, LT Kong and JH Liu. A facile precipitation synthesis of mesoporous 2-line ferrihydrite with good fluoride removal properties. *RSC Adv*. 2015; **103**, 84389-97.
[37] MG Peleyeju, EH Umukoro, L Tshwenya, R Moutloali, JO Babalola and OA Arotiba. Photoelectrocatalytic water treatment systems: Degradation, kinetics and intermediate products studies of sulfamethoxazole on a TiO_2-exfoliated graphite electrode. *RSC Adv.* 2017; **7**, 40571-80.
[38] S Bashir, RW McCabe, C Boxall, MS Leaver, and D Mobbs. Synthesis of α- and β-FeOOH iron oxide nanoparticles in non-ionic surfactant medium. *J. Nanopart. Res.* 2009; **3**, 701-6.
[39] B Yuan, J Xu, X Li and ML Fu. Preparation of Si-Al/α-FeOOH catalyst from an iron-containing waste and surface-catalytic oxidation of methylene blue at neutral pH value in the presence of H_2O_2. *Chem. Eng. J.* 2013; **226**, 181-8.
[40] A Munyengabe, C Zvinowanda, J Ramontja and JN Zvimba. Effective desalination of acid mine drainage using an advanced oxidation process: Sodium ferrate (VI) salt. *Water* 2021; **19**, 2619.
[41] A El Maghraoui, A Zerouale and M Ijjaali. Effect of degree of ClO^- hypochlorite on the wet synthesis of ferrate (VI). *Adv. Mater. Phys. Chem.* 2015; **5**, 133-9.
[42] D Kowalczuk, M Miazga-Karska, A Gładysz, P Warda, A Barańska and B Drop. Characterization of ciprofloxacin-bismuth-loaded antibacterial wound dressing. *Molecules* 2020; **21**, 5096.

[43] A Woziwodzka, M Krychowiak-Maśnicka, G Gołuński, A Łosiewska, A Borowik, D Wyrzykowski and J Piosik. New life of an old drug: Caffeine as a modulator of antibacterial activity of commonly used antibiotics. *Pharmaceuticals* 2022; **7**, 872.
[44] F Eldin, O Suliman and SM Sultan. Sequential injection technique employed for stoichiometric studies, optimization and quantitative determination of some fluoroquinolone antibiotics complexed with iron (III) in sulfuric acid media. *Talanta* 1996; **4**, 559-68.
[45] K Basavaiah, P Nagegowda, BC Somashekar and V Ramakrishna. Spectrophotometric and titrimetric determination of ciprofloxacin based on reaction with cerium (IV) sulphate. *ScienceAsia* 2006; **4**, 403-9.
[46] MH Abdel-Hay, EM Hassan, AA Gazy and TS Belal. Kinetic spectrophotometric analysis and spectrofluorimetric analysis of ciprofloxacin hydrochloride and norfloxacin in pharmaceutical preparations using 4-chloro-7-nitrobenzo-2-oxa-1, 3-diazole (NBD-Cl). *J. Chin. Chem. Soc.* 2008; **4**, 818.
[47] M Rizk, F Belal, F Ibrahim, S Ahmed and ZA Sheribah. Derivative spectrophotometric analysis of 4-quinolone antibacterials in formulations and spiked biological fluids by their Cu(II) complexes. *J. AOAC Int.* 2001; **2**, 368-75.
[48] M Thakur, S Pandey, A Mewada, V Patil, M Khade, E Goshi, and M Sharon. Antibiotic Conjugated Fluorescent Carbon Dots as a Theranostic Agent for Controlled Drug Release, Bioimaging, and Enhanced Antimicrobial Activity. *J. Drug Deliv*. 2014; **2014**, 282193.
[49] EA Serna-Galvis, F Ferraro, J Silva-Agredo and RA Torres-Palma. Degradation of highly consumed fluoroquinolones, penicillins and cephalosporins in distilled water and simulated hospital wastewater by UV254 and UV254/persulfate processes. *Water Res.* 2017; **122**, 128-38.
[50] T Ahamad, M Naushad and SM Alshehri. Analysis of degradation pathways and intermediates products for ciprofloxacin using a highly porous photocatalyst. *Chem. Eng. J.* 2021; **417**, 127969.
[51] J Deng, G Wu, S Yuan, X Zhan, W Wang and ZH Hu. Ciprofloxacin degradation in UV/chlorine advanced oxidation process: Influencing factors, mechanisms and degradation pathways. *J. Photochem. Photobiol. A Chem.* 2019; **371**, 151-8.
[52] HG Guo, NY Gao, WH Chu, L Li, YJ Zhang, JS Gu, and YL Gu. Photochemical degradation of ciprofloxacin in UV and UV/H_2O_2 process: Kinetics, parameters, and products. *Environ. Sci. Pollut. Res.* 2013; **5**, 3202-13.
[53] MER Jalil, M Baschini and K Sapag. Influence of pH and antibiotic solubility on the removal of ciprofloxacin from aqueous media using montmorillonite. *Appl. Clay Sci.* 2015; **114**, 69-76.
[54] M Zupančič, I Arčon, P Bukovec and A Kodre. A physico-chemical study of the interaction of cobalt (II) ion with ciprofloxacin. *Croat. Chem. Acta* 2002; **1**, 1-12.
[55] TA Gad-Allah, MEM Ali, and MI Badawy. Photocatalytic oxidation of ciprofloxacin under simulated sunlight. *J. Hazard. Mater.* 2011; **1**, 751-5.
[56] JC Durán-Álvarez. Synthesis and Characterization of the All Solid Z-Scheme Bi_2WO_6/Ag/AgBr for the photocatalytic degradation of ciprofloxacin in water. *Top Catal*. 2019; **12-16**, 1011-25.
[57] AS Giri and AK Golder. Ciprofloxacin degradation from aqueous solution by Fenton oxidation: Reaction kinetics and degradation mechanisms. *RSC Adv*. 2014; **13**, 6738-45.
[58] R Wajahat, A Yasar, AM Khan, AB Tabinda and SG Bhatti. Ozonation and Photo-Driven Oxidation of Ciprofloxacin in Pharmaceutical Wastewater: Degradation kinetics and energy requirements. *Pol. J. Environ. Stud.* 2019; **3**, 1933-8.
[59] S Badal, YF Her and LJ Maher. Nonantibiotic effects of fluoroquinolones in mammalian cells. *J. Biol. Chem.* 2015; **290**, 22287-97.
[60] CA Aggelopoulos, M Hatzisymeon, D Tataraki and G Rassias. Remediation of ciprofloxacin-contaminated soil by nanosecond pulsed dielectric barrier discharge plasma: Influencing factors and degradation mechanisms. *Chem. Eng. J.* 2020; **393**, 124768.
[61] HG Guo, NY Gao, WH Chu, L Li, YJ Zhang, JS Gu and YL Gu. Photo-chemical Degradation of Ciprofloxacin in UV and UV/H_2O_2 Process: Kinetics, Parameters, and Products. *Environ. Sci. Pollut. Res.* 2013; **5**, 3202-13.
[62] W Karl, J Schneider and HG Wetzstein. Outlines of an exploding network of metabolites generated from the fluoroquinolone enrofloxacin by the brown rot fungus gloeophyllum striatum. *Appl. Microbiol. Biotechnol.* 2006; **1**, 101-13.
[63] AS Giri and AK Golder. Ciprofloxacin degradation from aqueous solution by fen-ton oxidation: reaction kinetics and degradation mechanisms. *RSC Adv.* 2014; **13**, 6738-45.

[64] CL Amorim, IS Moreira, AS Maia, ME Tiri-tan and PM Castro. Biodegradation of ofloxacin, norfloxacin, and ciprofloxacin as single and mixed substrates by Labrys portucalensis F11. *Appl. Microbiol. Biotechnol.* 2014; **7**, 3181-90.

[65] VS Antonin, MC Santos, S Garcia-Segura and E Brillas. Electrochemical incineration of the antibiotic ciprofloxacin in sulfate medium and synthetic urine matrix. *Water Res.* 2015; **83**, 31-41.

[66] GE Ukpo, MA Owolabi, NOA Imaga, OO Oribayo and AJ Ejiroghene. Effect of *Carica papaya* (Linn) aqueous leaf extract on pharmacokinetic profile of ciprofloxacin in rabbits. *Trop. J. Pharm. Res.* 2017; **1**, 127-34.